

Loss of aquaporin 4 in lesions of neuromyelitis optica: distinction from multiple sclerosis

T. Misu,¹ K. Fujihara,¹ A. Kakita,² H. Konno,³ M. Nakamura,¹ S. Watanabe,¹ T. Takahashi,¹ I. Nakashima,¹ H. Takahashi² and Y. Itoyama¹

¹Department of Neurology, Tohoku University School of Medicine, Sendai, ²Department of Pathology and the Resource Branch for Brain Research CBBR, Brain Research Institute, Niigata University, Niigata and ³Department of Neurology, National Nishitaga Hospital, Sendai, Japan

Correspondence to: Dr Tatsuro Misu, MD, Department of Neurology, Tohoku University School of Medicine, 1-1 Seiryomachi, Aobaku, Sendai 980-8574, Japan

E-mail: misu@em.neurol.med.tohoku.ac.jp

Neuromyelitis optica (NMO) is an inflammatory and necrotizing disease clinically characterized by selective involvement of the optic nerves and spinal cord. There has been a long controversy as to whether NMO is a variant of multiple sclerosis (MS) or a distinct disease. Recently, an NMO-specific antibody (NMO-IgG) was found in the sera from patients with NMO, and its target antigen was identified as aquaporin 4 (AQP4) water channel protein, mainly expressed in astroglial foot processes. However, the pathogenetic role of the AQP4 in NMO remains unknown. We did an immunohistopathological study on the distribution of AQP4, glial fibrillary acidic protein (GFAP), myelin basic protein (MBP), activated complement C9neo and immunoglobulins in the spinal cord lesions and medulla oblongata of NMO ($n=12$), MS ($n=6$), brain and spinal infarction ($n=7$) and normal control ($n=8$). The most striking finding was that AQP4 immunoreactivity was lost in 60 out of a total of 67 acute and chronic NMO lesions (90%), but not in MS plaques. The extensive loss of AQP4 accompanied by decreased GFAP staining was evident, especially in the active perivascular lesions, where immunoglobulins and activated complements were deposited. Interestingly, in those NMO lesions, MBP-stained myelinated fibres were relatively preserved despite the loss of AQP4 and GFAP staining. The areas surrounding the lesions in NMO had enhanced expression of AQP4 and GFAP, which reflected reactive gliosis. In contrast, AQP4 immunoreactivity was well preserved and rather strongly stained in the demyelinating MS plaques, and infarcts were also stained for AQP4 from the very acute phase of necrosis to the chronic stage of astrogliosis. In normal controls, AQP4 was diffusely expressed in the entire tissue sections, but the staining in the spinal cord was stronger in the central grey matter than in the white matter. The present study demonstrated that the immunoreactivities of AQP4 and GFAP were consistently lost from the early stage of the lesions in NMO, notably in the perivascular regions with complement and immunoglobulin deposition. These features in NMO were distinct from those of MS and infarction as well as normal controls, and suggest that astrocytic impairment associated with the loss of AQP4 and humoral immunity may be important in the pathogenesis of NMO lesions.

Keywords: neuromyelitis optica; multiple sclerosis; aquaporin 4; astrocyte; necrosis

Abbreviations: GFAP = glial fibrillary acidic protein; AQP4 = aquaporin 4; BBB = blood–brain barrier; LCA = leucocyte antigen; MBP = myelin basic protein; PLP = proteolipid protein; VEGF = vascular endothelial growth factor

Received November 10, 2006. Revised February 12, 2007. Accepted February 13, 2007. Advance Access publication April 2, 2007

Introduction

Neuromyelitis optica (NMO) is an idiopathic inflammatory, necrotizing disease characterized by selective involvement of the optic nerves and spinal cord (Clyos and Netsky, 1970; Kuroiwa, 1985). Both monophasic and relapsing NMO have been known since the original description (Devic, 1894, Gault, 1895). Relapsing NMO

has been called optic-spinal multiple sclerosis (OSMS) in Japan and other Asian countries (Kuroiwa, 1985; Misu *et al.*, 2002). It has long been controversial whether NMO or Devic's disease is a variant of MS or a distinct disease. Recently, a number of distinctive clinical and laboratory features of relapsing NMO and OSMS differing from

classical MS have been identified such as female-predominance, low frequencies of oligoclonal IgG band, longitudinally extensive (>3 vertebral segments) spinal cord lesions, polymorphonuclear cell-dominant pleocytosis, and poor clinical prognosis with blindness, tetraparesis and respiratory failure (Mandler *et al.*, 1993; Wingerchuk *et al.*, 1999; Misu *et al.*, 2002; Kira, 2003). Neuropathological studies in NMO showed that tissue necrosis often associated with cavity formation and grey matter involvement was evident in addition to demyelination (Cloys and Netsky, 1970; Kuroiwa, 1985). Moreover, humoral immunity such as the perivascular deposition of immunoglobulin and complement, and the infiltration of neutrophils or eosinophils, were the dominant immunopathological features in the lesions of NMO (Mandler *et al.*, 1993; Lucchinetti *et al.*, 2002). In Japanese OSMS, it was reported that there were necrotic lesions with a loss of glial fibrillary acidic protein (GFAP) staining in the spinal cord lesions, but the mechanism of the astroglial defect has remained unknown (Itoyama *et al.*, 1985).

Recently, a disease-specific autoantibody, NMO-IgG, was found in the sera from patients with Caucasian NMO and Japanese OSMS patients (Lennon *et al.*, 2004). Subsequently, it was found that NMO-IgG bound selectively to aquaporin 4 (AQP4) water channel (Lennon *et al.*, 2005), which is densely expressed in astrocytic foot processes at the blood–brain barrier (BBB) (Jung *et al.*, 1994). Very recently, we reported a case of typical NMO which showed a loss of AQP4 immunostaining in the spinal cord lesions, especially in active perivascular lesions (Misu *et al.*, 2006). Such a loss of AQP4 has not been found in demyelinating lesions of MS. Therefore, in the present study, we performed immunohistochemical analyses

of AQP4 in more NMO cases to clarify whether the loss of AQP4 immunostaining in lesions commonly occurs in NMO lesions and is a distinctive pathological feature of NMO from MS and brain and spinal cord infarction.

Material and methods

Autopsied cases of NMO, MS and other neurological disorders

In the present study, we analysed 12 cases of NMO and 6 cases of MS. The clinical findings of the patients are summarized in Table 1. The median age was 52.5 (range 19–80) years in NMO (8 females and 4 males) and 46 (range 22–67) years in MS (3 females and 3 males). Disease durations ranged from 0.3 to 28 years in NMO (median, 3 years) and from 3 to 21 years in MS (median, 9.75 years). The clinical course of NMO was relapsing in 10 patients and monophasic in 2 patients. The diagnosis of NMO was made only by clinical manifestations (Wingerchuk *et al.*, 1999). The diagnosis of MS was made according to the Poser criteria (Poser *et al.*, 1983).

In addition, as neurological and non-neurological controls, we studied 10 lesions of infarction including cerebral infarction in acute phase ($n=3$) (two basal ganglia lesions and one subcortical lesion), cerebral infarction in chronic phase ($n=5$) (one brainstem lesion, one occipital artery occlusion, two basal ganglia lesions and one subcortical lesion), two chronic spinal cord lesions of Foix–Alajouanine syndrome ($n=2$), an angiodysgenetic necrotizing myelopathy and eight spinal cords of non-neurological and non-inflammatory diseases ($n=8$).

Neuropathological techniques and immunohistochemistry

The spinal cords and brains of the cases and the optic nerve of a single case of NMO (NMO12) were processed for

Table 1 Summary of clinical findings of patients with neuromyelitis optica (NMO) and multiple sclerosis (MS)

Case	Age (years), sex	Disease duration (years)	Duration after last attack	Clinical exacerbations
NMO1	67, F	3	2 months	O2, S2
NMO2	65, F	28	7 months	O6, S5, Bs2
NMO3	46, F	8	2 months	O2, S1, Bs1
NMO4	51, M	12	1 month	O1, S3, Bs3
NMO5	54, F	1.8	6 months	O1, S1
NMO6	37, F	0.8	1 week	O3, S2
NMO7	19, F	5	2 months	O6, S3
NMO8	68, F	3	9 months	O1, S3
NMO9	36, F	2	2 weeks	O1, S1, Bs6
NMO10	80, M	0.8	2 weeks	O1, S1, Bs1
NMO11	77, M	0.3	2 months	O1, Bs1
NMO12	43, F	20	2 weeks	O5, S6, Cr1
MS1	56, F	21	3 years	S10, Cr2
MS2	38, M	10	7 months	O1, S1, Cr2
MS3	54, M	9.5	2 years	O2, S3, Cr6
MS4	31, F	13	2 years	O2, S3, Cr6
MS5	67, F	3	4 months	S2, Cr1
MS6	22, M	3	10 months	O3, S2, Cr3

Sites of lesion in clinical exacerbations are as follows: O, optic; S, spinal; Bs, brainstem; Cr, cerebral or cerebellar. The numbers attached to clinical exacerbations mean the counts of exacerbations in each lesion site. (ex. O2 represents two episodes of optic neuritis.)

paraffin-embedded to routine procedures. Tissue slices of 5–6 μm thickness were cut and mounted serially on numbered slides so that the distribution of molecules such as AQP4, GFAP and myelin components were compared in adjacent serial sections. We stained all sections with haematoxylin and eosin (HE), Klüver–Barrera (KB) and Bodian staining.

We used the immunostaining system of avidin–biotinylated enzyme complex (ABC) (Vectastain, Vector, CA) or EnVision (DAKO, Carpinteria, CA). Briefly, at first the paraffin sections on slides were immersed in xylene for 5 min three times, and then they were immersed in 100% ethanol, 95% ethanol and then 90% ethanol for 5 min each. After washing with distilled water, we washed the slides three times with phosphate buffered saline (PBS). Non-specific binding was blocked with 10% goat serum for 15 min at room temperature, and the slides were covered with the primary antibodies listed in Table 2 and incubated for 1–48 h at the appropriate temperature. The primary antibody was omitted in the control study. Then, the slides were washed with PBS and incubated with PBS containing 30% methanol and 1 ml of H_2O_2 (30%) for 20 min followed by washing three times with PBS. Secondary antibodies were applied and incubated for 45 min to 1 h at room temperature according to the manufacturer's protocols. For staining, we used diaminobenzidine hydrochloride (DAB) (brown) for the horseradish peroxidase (HRP) system, and fuchsin (DAKO, Carpinteria, CA) (red) or Vector blue (Vector, CA) (blue) for the alkaline phosphatase (AP) system. Selected sections were counterstained with a filtered solution of haematoxylin (blue), methyl green (Vector) (green) or fast nuclear red (Vector) (red).

For double staining, we combined two enzyme systems, HRP and AP. For example, in the double staining of MBP and C9neo, we first applied mouse anti-human C9neo antibody and then incubated with HRP-conjugated anti-mouse IgG and stained by DAB according to the single staining procedure. After washing

three times with PBS, we further applied rabbit anti-human MBP antibody and then incubated with AP-conjugated anti-rabbit IgG and stained by Vector blue. Counterstaining was done by methyl green or nuclear fast red, where applicable. The slides were mounted with VectaMount (Vector).

Lesion staging

We classified the lesions of NMO and MS into the following four stages (1–4):

(1) Acute inflammatory lesions, (2) actively demyelinating lesions, (3) chronic active lesions and (4) chronic inactive lesions.

'Actively demyelinating', 'chronic active' and 'chronic inactive' lesions were based on the histological staging criteria for MS lesions (Lassmann *et al.*, 1998; Trapp *et al.*, 1998), and we added 'acute inflammatory' lesions as the most acute phase of the disease, referring to the Vienna consensus (Lassmann *et al.*, 1998). Acute inflammatory lesions are infiltrated with numerous perivascular mononuclear and/or polymorphonuclear cells with relatively small numbers of macrophages seen in the clinically acute phase (within 2 weeks of relapse onset). Actively demyelinating lesions are diffusely infiltrated by macrophages containing myelin debris stained by KB staining. Chronic active lesions are hypocellular at the lesion centre and hypercellular at the lesion rim (the main component of the cellularity is macrophage/microglia). Chronic inactive lesions are hypocellular throughout the entire lesions.

According to this staging protocol, NMO lesions ($n=67$, 59 spinal cord lesions and 8 medullary lesions) were classified into 22 acute inflammatory lesions, 25 actively demyelinating lesions, 8 chronic active lesions and 12 chronic inactive lesions. MS lesions ($n=10$) were classified into one actively demyelinating lesion, five chronic active lesions and four chronic inactive lesions.

In each lesion, we judged the immunoreactivity of AQP4, GFAP and MBP as completely lost (lost) or partially preserved

Table 2 The list of antibodies used

Antigen	Dilution	Type	Clone (Lot. No.)	Company/provider
Macrophage/microglia				
CD45LCA	1 : 1	mouse	D7/26 and 2BIID	DAKO
CD68	1 : 1	mouse	KPI	DAKO
Myelin/oligodendrocytes				
MBP	1 : 1	rabbit	NI546	DAKO
PLP	1 : 100	mouse	plp1	Serotec
Peripheral myelin Po	1 : 2000	mouse	P07	Dr Archelos (Astexx Ltd)
Astrocytes				
GFAP	1 : 50	mouse	6F2	Monosan
GFAP	1 : 500	rabbit	Z0334	DAKO
Aquaporin				
Aquaporin 4	1 : 500	rabbit	AB3594	Chemicon Int.
Aquaporin 1	1 : 500	rabbit	AB3272	Chemicon Int.
Immunoglobulin and complement				
IgG	1 : 500	rabbit	A0423	DAKO
IgM	1 : 300	rabbit	A0425	DAKO
C9neo	1 : 100	mouse	B7	Dr Morgan BP
Other antibodies				
VEGF	1 : 100	mouse	VGI	NeoMarkers
CD31	1 : 20	mouse	JC70A	DAKO
Neurofilament	1 : 1	mouse	2FII	DAKO

LCA = leucocyte antigen, MBP = myelin basic protein, PLP = proteolipid protein, GFAP = glial fibrillary acidic protein, VEGF = vascular endothelial growth factor, CD31 = an endothelial cell marker.

(preserved), and divided the main expression patterns of the three molecules in each lesion into the following six patterns: Pattern A (AQP4-lost, GFAP-lost and MBP-preserved), B (AQP4-lost, GFAP-lost and MBP-lost), C (AQP4-lost, GFAP-preserved and MBP-preserved), D (AQP4-lost, GFAP-preserved and MBP-lost), E (AQP4-preserved, GFAP-preserved and MBP-lost) and F (AQP4-preserved, GFAP-preserved and MBP-preserved).

Results

AQP4 and GFAP expression pattern in the spinal cord of normal controls

In the cervical cord of normal control subjects (eight cases), AQP4 was diffusely expressed in the entire cord area, but the staining was stronger in the central grey matter than in the white matter (Fig. 1A). In the grey matter, dense, fine, fibrous structures were stained for AQP4. In the white matter, the fine structures corresponding to radial blood vessels and pia mater were also strongly stained for AQP4 (Fig. 1B) and GFAP (Fig. 1C).

Neuropathological and immunohistochemical findings in NMO

General neuropathological findings of NMO lesions

In the spinal cords with NMO lesions, extensive inflammation with oedema, necrosis with cystic changes or cavitation and cord atrophy were commonly seen. With high magnification, inflammatory lesions with or without necrotic changes were often located in the perivascular regions, where there were perivascular cuffing of mononuclear and polymorphonuclear cells (in the clinically acute phase), infiltration of macrophages and microvessel proliferation around small vessels with thickened walls. Thirty-five (59%) out of 59 spinal cord NMO lesions occupied over half the area of the spinal cord sections.

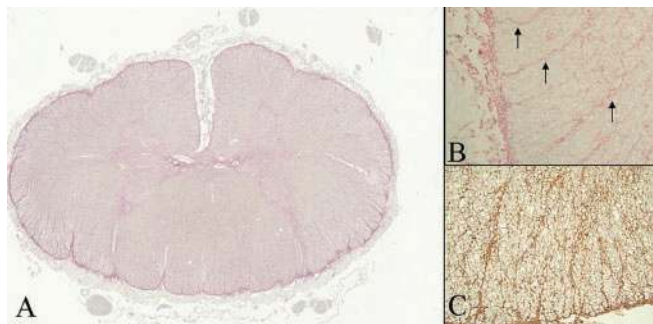


Fig. 1 Expression and distribution of aquaporin-4 (AQP4) and glial fibrillary acidic protein (GFAP) in the normal spinal cord. **(A)** The central grey matter was diffusely positive for AQP4 (pink). Radial vessels running from the central grey matter to the cord surface were positive for AQP4. **(B)** With high magnification, fine structures corresponding to astrocytic foot processes (arrow) and the pia mater were positive for AQP4 (mag $\times 200$). **(C)** Fine structures positive for GFAP were also positive for AQP4, corresponding to the vascular foot processes of astrocytes (mag $\times 200$).

In contrast, in MS, the spinal cord lesions were relatively small, and 6 out of 10 cord lesions were mainly localized in the white matter. Peripheral rims of the cord were relatively spared in all NMO cases, while demyelinating plaques in MS involved the periphery of the cord.

In the cerebral and cerebellar hemispheres of NMO, there were absolutely no lesions in four cases and only a few, small, ischaemic or demyelinating white matter lesions except two cases with multiple or diffuse lesions (NMO7 and NMO12). In the medulla oblongata, there were eight NMO cases with acute inflammatory and active demyelinating lesions, with cystic changes as described in the spinal cord lesions of NMO. The optic nerve from a single case of NMO also had a similar acute inflammatory lesion with necrosis and cysts (data not shown).

Immunohistochemical findings of NMO lesions

Immunohistochemical pattern of AQP4, GFAP and MBP in four NMO lesion stages. As summarized in Table 3, the NMO lesions were subdivided into ‘acute inflammatory’ (22 lesions), ‘actively demyelinating’ (25 lesions), ‘chronic active’ (8 lesions) and ‘chronic inactive’ (12 lesions) types.

In the acute inflammatory lesions, relatively preserved myelin with complete loss of AQP4 and GFAP (Pattern A) was the main feature (73%), and AQP4 was lost in all lesions (100%). The loss of AQP4 accompanied by the loss of GFAP staining (Patterns A and B) was evident in 86% of the lesions. In actively demyelinating lesions, the expression patterns of GFAP and MBP were varied (Patterns A–D), but AQP4 was lost in all but one lesion (96%). The loss of AQP4 accompanied by the loss of GFAP staining (Patterns A and B) was seen in 56% of the lesions. In chronic active lesions, cystic AQP4-negative lesions (88%) with mild macrophage infiltration were surrounded by astrocytes and many macrophages. In chronic inactive lesions, the lesions were hypocellular and were often severely necrotic, and were cystic with the loss of AQP4 and MBP but showed partially preserved GFAP immunoreactivity (Pattern D) (50%) except some AQP4- and GFAP-faintly positive lesions (Patterns E and F).

Acute inflammatory lesions (Table 3). In acute inflammatory lesions (Fig. 2), Pattern A was the most common. In these lesions, AQP4 immunoreactivity was completely lost in extensive regions, especially in the lesion cores and in the perivascular areas along the radial blood vessels in the white matter where perivascular depositions of complement C9neo were present (Fig. 2A and D). In some lesions, loss of AQP4 immunoreactivity extended to the cord rim beneath the pia mater. Immunoreactivity for GFAP was also largely lost or decreased (Fig. 2B) in the lesions, and they were often surrounded by areas with stronger GFAP staining (Fig. 2B) than that in control white matter (Fig. 1C). As shown in Fig. 2A, perivascular white matter lesions lacking AQP4 around C9neo-stained vessels,

Table 3 The patterns of aquaporin 4, glial fibrillary acidic protein, and myelin basic protein expression in lesions of neuro-myelitis optica

Lesion pattern	Lesion staging			Lesion staging			
	AQP4	GFAP	MBP	Acute inflammatory (n = 22)	Active demyelinating (n = 25)	Chronic active (n = 8)	Chronic inactive (n = 12)
Pattern A	(-)	(-)	(+)	16	7	3	0
Pattern B	(-)	(-)	(-)	3	7	0	1
Pattern C	(-)	(+)	(+)	2	4	0	0
Pattern D	(-)	(+)	(-)	1	6	4	6
Pattern E	(+)	(+)	(-)	0	1	1	3
Pattern F	(+)	(+)	(+)	0	0	0	2

AQP4 = aquaporin 4, GFAP = glial fibrillary acidic protein, MBP = myelin basic protein. (-): complete loss of immunoreactivity, (+): partially preserved immunoreactivity.

were surrounded by AQP4-rich reactive astrogliosis. The pattern of the perivascular loss of GFAP immunoreactivity surrounded by areas with diffusely increased GFAP immunoreactivity (Fig. 2B) was essentially similar to the findings of AQP4 (Fig. 2A).

On the other hand, MBP-stained myelinated fibres were relatively preserved in those lesions (Fig. 2C). These preserved myelinated fibres were not stained with P0 antibody. In a more severely destroyed lesion (Fig. 2E and F) lacking AQP4 and GFAP, P0 stained myelinated fibres were seen in the part of the dorsal portion of the cord as we previously reported (Itoyama *et al.*, 1985).

With high magnification of double staining with MBP and C9neo, MBP immunostaining was remarkably decreased at the lesion core (Fig. 2G), and was also partially decreased at the periphery of the perivascular C9neo-deposited lesion lacking AQP4 and GFAP (Fig. 2H), but myelinated fibres without thinly remyelinating changes or myelin debris were seen at the periphery of C9neo-positive or negative areas (Fig. 2H and I), suggesting myelin preservation. In addition, there was axonal loss evidenced by neurofilament debris in the lesion core (Fig. 2J).

Actively demyelinating lesions and chronic lesions (Table 3). In actively demyelinating lesions, the expression patterns of AQP4, GFAP and MBP were heterogeneous, including Pattern A, which was commonly seen in acute inflammatory lesions. However, as compared with other lesion stages, demyelinating lesions with numerous myelin-debris-laden macrophages and thinly myelinated fibres (Pattern C) (AQP4-completely lost, GFAP- and MBP-partially preserved) were relatively common in actively demyelinating lesions. Pattern A was also observed in chronic active lesions. Patterns D and E were essentially associated with cystic necrosis. Diffuse cystic lesions with various degrees of macrophage infiltration where myelin was absolutely lacking (Pattern D), were commonly seen in chronic active and chronic inactive lesions as well as in actively demyelinating lesions. Some lesions in the late stage showed partially restored AQP4 immunoreactivity (Pattern

E). Lesions with preserved immunoreactivity of AQP4, GFAP and MBP (Pattern F) were seen only in chronic inactive lesions.

Perivascular depositions of complements, immunoglobulins and VEGF in NMO. At the perivascular lesions lacking AQP4 (Fig. 3A), there were fine structures stained for GFAP whose immunoreactivity was weaker than that of perivascular astrocytic foot processes in normal controls (Fig. 1C), around dilated blood vessel walls (Fig. 3B), and this area was surrounded by reactive astrogliosis positive for AQP4 and GFAP.

With high magnification (Fig. 3C), those GFAP-weakly positive fine structures, probably corresponding to astrocytic foot processes, appeared partially swollen and were observed as rosette-like formations which were also stained with C9neo (Fig. 3D), IgM (Fig. 3E), IgG (Fig. 3F) or VEGF (Fig. 3G) deposited in the perivascular fine structures. Such perivascular deposits of immunoglobulins and complements were observed to be much milder and were less frequently seen in cases of MS and were never encountered in normal controls. VEGF deposition was detected in active lesions.

Immunohistochemical findings of MS lesions and infarctions (Table 4)

The immunohistochemical features of MS lesions (Fig. 4A–E) were quite different from those of NMO lesions (Fig. 4F–J). The lesions in our cases of MS were chronic active or chronic inactive lesions or active demyelinating lesions, and demyelinating plaques were sharply demarcated as areas with the loss of MBP staining with infiltration of macrophages, especially in the lesion rim, and a small amount of myelin debris, but there was no area where AQP4 (Fig. 4A) and GFAP (Fig. 4B) immunoreactivities were lost, and GFAP was stained diffusely in demyelinated (Fig. 4C) and normal appearing white matter (Fig. 4B). Most lesions were partially remyelinated (Pattern F). These features in MS were distinct from those of the NMO lesions including the chronic active and

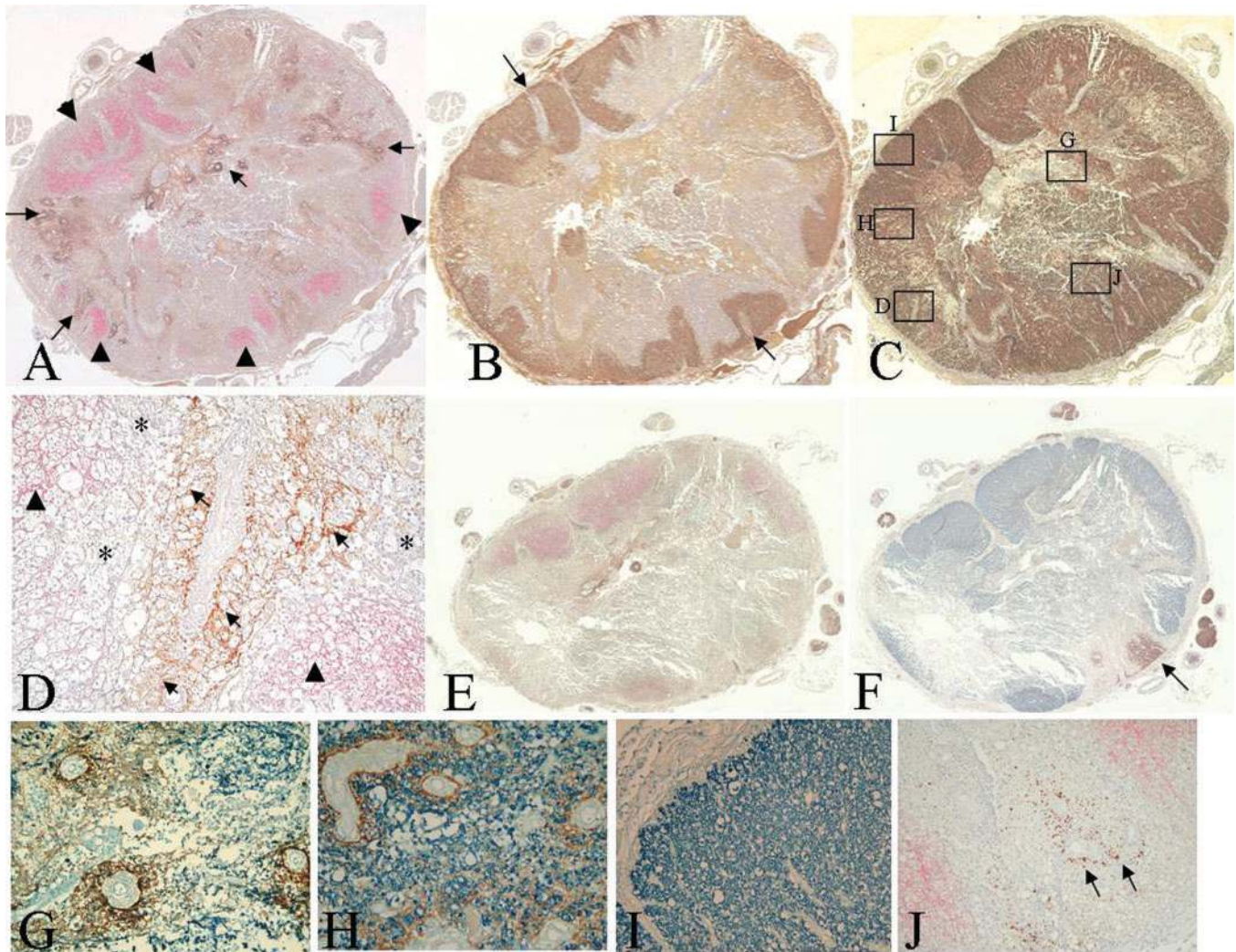


Fig. 2 Loss of aquaporin 4 (AQP4) and glial fibrillary acidic protein (GFAP) but relatively preserved myelin basic protein (MBP) in neuro-myelitis optica (NMO) lesions. **(A)** Spinal cord sections demonstrating extensive necrotic and cavitory lesions especially at the central portion of the cervical cord (NMOI2). **(A)**, **(B)** and **(C)** are serial sections. AQP4 (pink, arrowheads) was diffusely lost and stained only at the periphery of the cord. In AQP4-lacking areas, activated complement C9neo was diffusely stained particularly around numerous dilated vessels (brown, arrows). **(B)** The staining pattern of GFAP was also preserved at the periphery of the cord and very faint or lost at the cavitory and necrotic lesions especially at the central portion of the cord and perivascular areas along radial vessels (arrows). **(C)** Myelin basic protein (MBP) was relatively well-preserved except for the partial loss of the immunoreactivity at the central grey matter and some perivascular regions of the white matter. Selected areas **(D, G, H, I** and **J)** of the lesion core and periphery are presented in more detail. **(D)** With high magnification, at the perivascular region with relatively preserved myelin, there were dilated vessels with depositions of activated complement C9neo (brown, arrows) in the centre surrounded by a strong mesh-like expression of AQP4 (pink, arrowheads). AQP4 was completely lacking in the region between them (*) (mag $\times 400$). **(E)** Another cervical cord section of the same patient had more severely destroyed lesions including extensive necrosis and large cystic changes with C9neo-positive vessels, and AQP4 expression was diminished particularly in the severely affected areas. **(F)** MBP staining was also decreased at the severely affected areas, but the stainings in other peripheral portions were relatively intact. Remyelination by peripheral myelin P0 (arrow) was limited to the posterior portion of this section. **(G)** In the central portion of the lesion, MBP-positive myelinated fibres were decreased around C9neo-positive (brown) dilated vessels (mag $\times 200$). **(H)** In C9neo-positive (brown) perivascular areas at the lesion periphery lacking AQP4 and GFAP, MBP-positive myelinated fibres were relatively preserved, but mildly decreased compared with the normal appearing white matter shown in **(I)** (mag $\times 200$). **(I)** Normal appearing white matter was strongly and diffusely positive for AQP4 and GFAP, but had no remyelinating signs of thinly myelinated fibres (mag $\times 200$). **(J)** There was some diffuse axonal loss at the lesions with no AQP4 staining (pink). Neurofilament densely positive deposits represent axonal debris (brown, arrows, mag $\times 100$).

actively demyelinating lesions (Fig. 4F–H) in that the lesions that included shadow plaques with partially preserved MBP staining were clearly identified by the complete loss of AQP4 and GFAP staining.

With high magnification, in MS, the pia mater and demyelinating lesions (Fig. 4D) were diffusely stained for GFAP as well as AQP4 (Fig. 4E) with many hypertrophic astrocytes and fibrous structures

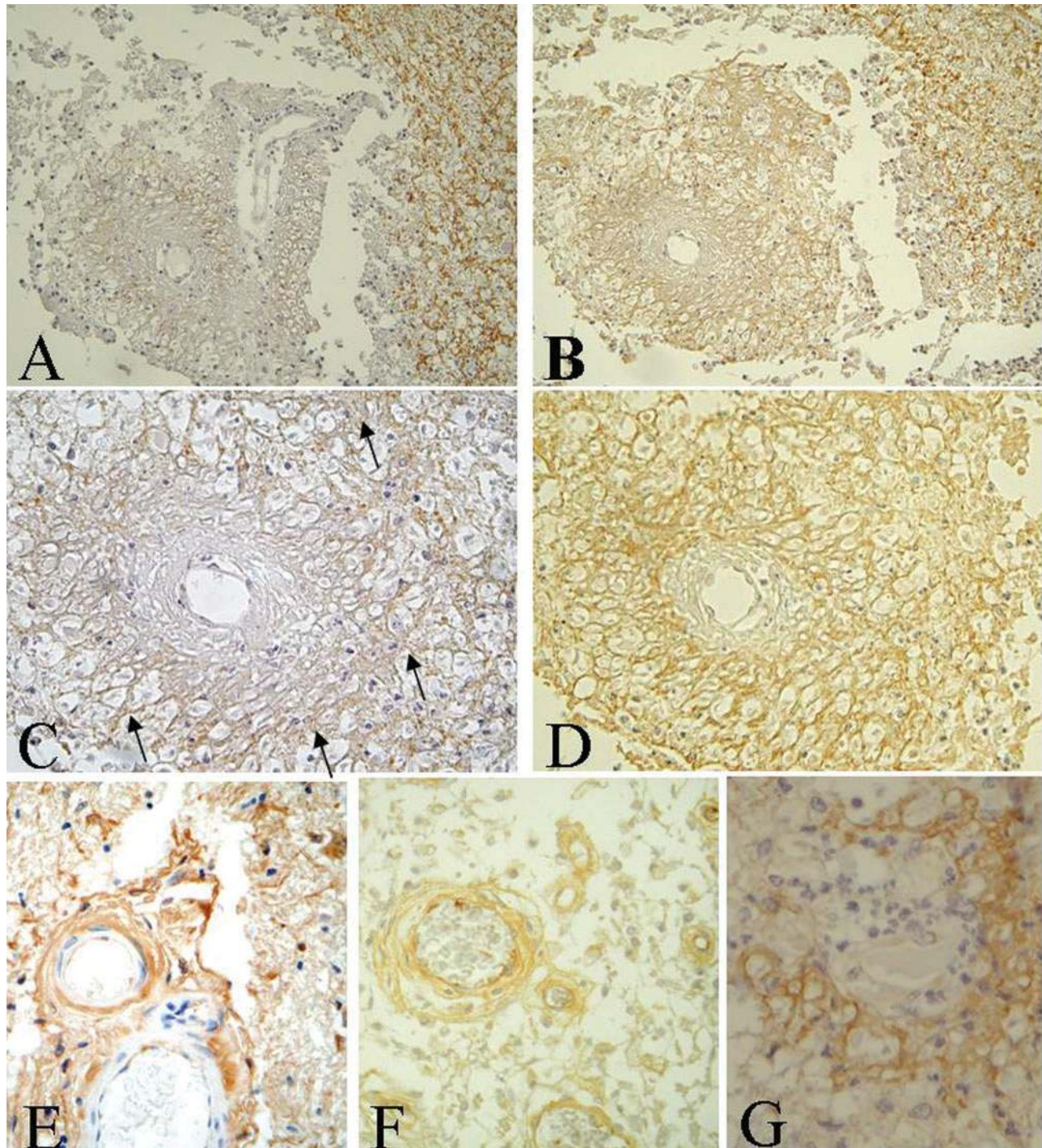


Fig. 3 Perivascular depositions of activated complements and immunoglobulins in dilated vessel in cavitory lesions. **(A)** and **(B)** are serial sections. In severely necrotic and perivascular lesions lacking AQP4 (mag $\times 100$), the areas surrounding the lesions were strongly positive for AQP4 **(A)** and GFAP **(B)** with astrocytic morphology. **(C)** and **(D)** are serial sections. **(C)** GFAP immunoreactivity was faint or negative (arrows) (mag $\times 400$), but GFAP-faintly positive structures corresponding to astrocytic feet were identifiable (arrows). **(D)** C9neo showed mesh-like or rosette-like formations (mag $\times 400$). **(E)** **(F)** and **(G)** Immunoglobulins, IgM **(E)** (mag $\times 400$) and IgG **(F)** (mag $\times 400$) and vascular endothelial growth factor (VEGF) **(G)** (mag $\times 1000$) were positive at the dilated vessels in the lesions.

corresponding to astrocytic foot processes. In contrast, only the edges of well-demarcated lesions in NMO were infiltrated with AQP4- and GFAP-stained hypertrophic astrocytes (Fig. 4I and J).

In acute basal ganglia infarction with only early necrotic signs of eosinophilic appearance and cellular cystic changes (Fig. 5A), AQP4 was stained across the whole area of the lesion (Fig. 5B), especially in the perivascular area (Fig. 5C).

Table 4 The patterns of aquaporin 4, glial fibrillary acidic protein, and myelin basic protein expression in the lesions of multiple sclerosis and infarction

Lesion pattern				Multiple sclerosis (n = 10)			Infarction (n = 10)	
	AQP4	GFAP	MBP	Active demyelinating (n = 1)	Chronic active (n = 5)	Chronic inactive (n = 4)	Acute (n = 3)	Chronic (n = 7)
Pattern A	(–)	(–)	(+)	0	0	0	0	0
Pattern B	(–)	(–)	(–)	0	0	0	0	3
Pattern C	(–)	(+)	(+)	0	0	0	0	0
Pattern D	(–)	(+)	(–)	0	0	0	0	2
Pattern E	(+)	(+)	(–)	1	1	1	1	1
Pattern F	(+)	(+)	(+)	0	4	3	2	1

AQP4 = aquaporin 4, GFAP = glial fibrillary acidic protein, MBP = myelin basic protein. (–): complete loss of immunoreactivity, (+): partial immunoreactivity.

In acute to chronic infarct lesions where necrotic changes were observed, AQP4 and GFAP were also positive as reactive astrogliosis (Fig. 5D), except in severe necrotic lesions with lost immunoreactivity of AQP4, GFAP and MBP (Table 4).

As described earlier, the complete loss of AQP4 from acute to chronic stages as seen in NMO were not observed in any cases of MS or infarction.

Discussion

We previously reported an immunohistochemical study of a case of NMO, in which the spinal cord lesions extended longitudinally from the cervical to thoracic cord (Misu *et al.*, 2006). In the spinal cord lesions, AQP4 staining was lost especially in the central grey matter of the spinal cord and was associated with the loss of or low GFAP immunoreactivity, while MBP-stained myelinated fibres were relatively preserved (Misu *et al.*, 2006). In the present study in which we examined 67 lesions from 12 cases of NMO, we confirmed the previous findings and clearly demonstrated unique immunocytochemical features in NMO lesions that were distinct from those in MS lesions. They are as follows: (1) NMO lesions were characterized by the loss of or impaired AQP4 and GFAP immunostaining from the early lesion stage (acute inflammatory lesions), (2) MBP stained myelinated fibres were relatively preserved in NMO lesions in the acute inflammatory and actively demyelinating phase, where immunocytochemical changes of AQP4 and GFAP were observed, (3) In MS lesions, neither AQP4 nor GFAP immunoreactivity was lost but was rather increased as compared with normal control white matters.

In MS, it is well-known that reactive astrogliosis is histologically prominent and its GFAP immunoreactivity is always upregulated in and around demyelinated plaques (Holley *et al.*, 2003; Ayers *et al.*, 2004). Recently, Aoki-Yoshino and her colleagues immunocytochemically studied MS lesions using antibody to AQP4. They demonstrated that AQP4 immunoreactivity was increased in lesions of MS as well as those of viral encephalitis.

AQP4-stained astrocytes were widely observed in the centre and the periphery of demyelinated MS plaques (Aoki-Yoshino *et al.*, 2005). Their results of AQP4 immunoreactivity in MS lesions were similar to our findings. Therefore, the immunohistochemical features in NMO lesions, especially the loss of AQP4 staining in the lesion, were quite unique to NMO.

AQP4 is abundant in the central nervous system, particularly in the grey matter of the spinal cord, the periventricular area and periaqueductal areas (Jung *et al.*, 1994; Oshio *et al.*, 2004). Also, this water channel protein is densely localized in the astrocytic foot processes (Vizuete *et al.*, 1999), and underlies the pia mater and the microvessels to form the BBB. Interestingly, the distribution of AQP4-rich areas in the central nervous system, such as the hypothalamus or the grey matter of the spinal cord, is compatible with that of NMO lesions (Misu *et al.*, 2005; Nakashima *et al.*, 2006; Pittock *et al.*, 2006). Moreover, in the present study, in NMO lesions the deposition of humoral factors was predominantly observed in perivascular areas, which are known to be occupied by astrocytic vascular feet and to be rich in AQP4. These findings strongly suggested that AQP4 might be involved in the pathogenesis of NMO.

We herein observed NMO lesions immunohistochemically as areas lacking both AQP4 and GFAP immunoreactivity. We previously reported cases of Japanese OSMS which had large spinal cord lesions lacking GFAP immunoreactivity, and those lesions were filled with Schwann cells and P0-stained remyelinated fibres (Itayama *et al.*, 1985). The lack of GFAP staining in those OSMS lesions was evident in the central portion of the spinal cords, which was similar to that found in the present study. Our previous and present findings strongly suggest that the loss of astrocytes or astrocytic impairment is closely related to the lesion formation in NMO.

The pathogenetic mechanisms for the loss or down-regulation of AQP4 and GFAP in NMO lesions remain to be elucidated. However, since the perivascular deposition of immunoglobulins and activated complements was found in

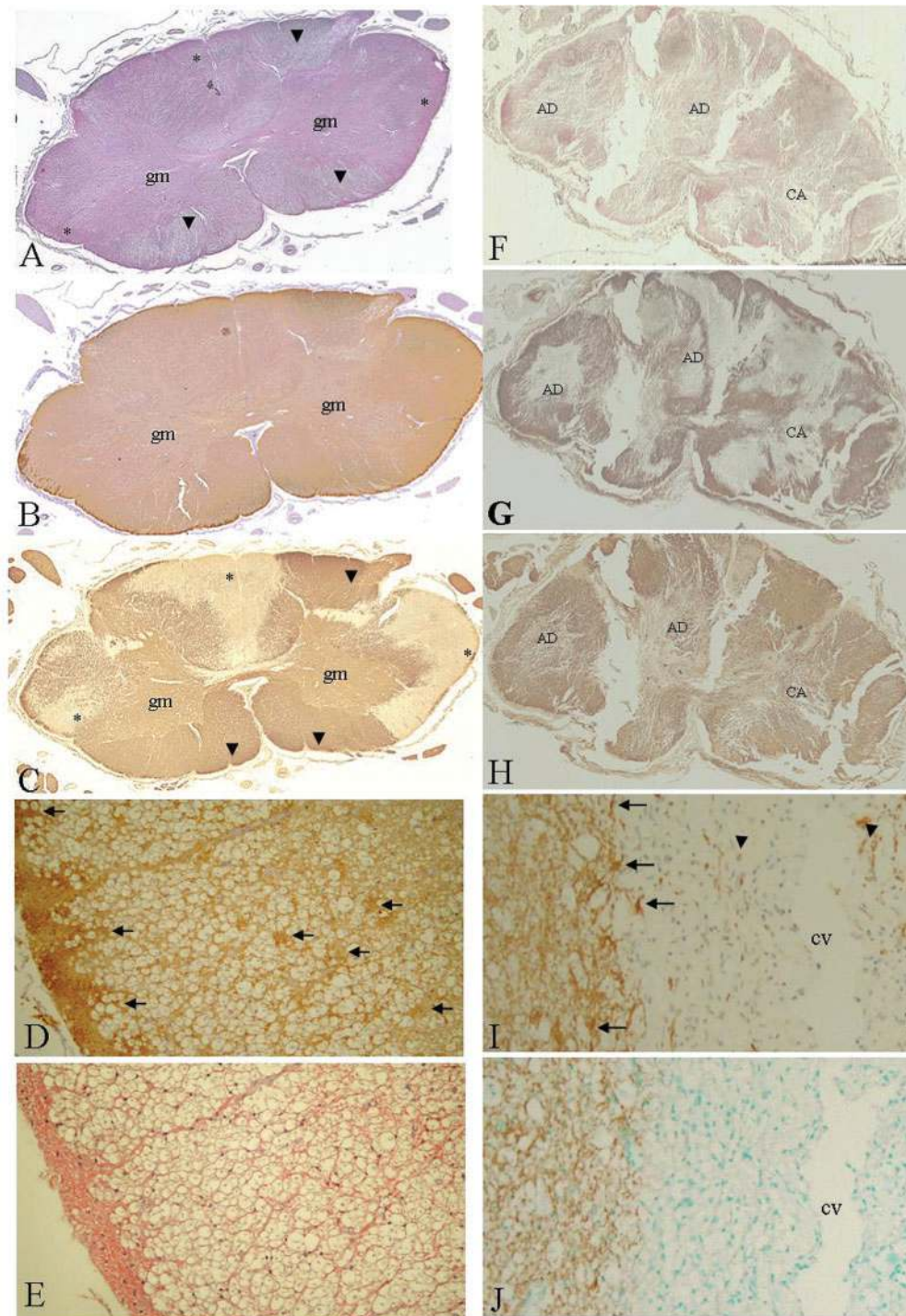


Fig. 4 Comparative immunohistochemical features of neuromyelitis optica (NMO) and multiple sclerosis (MS). The aquaporin-4 (AQP4), glial fibrillary acidic protein (GFAP) and myelin basic protein (MBP)-staining patterns of the spinal cord lesions in typical MS (**A** to **C**). (**A** to **C**) are serial sections of MS2. (**A**) In MS plaques (chronic active lesions) (*) shown in (**C**) with MBP staining, AQP4 was strongly stained pink, especially at the pia mater (*), but non-demyelinated areas (arrowheads) were not or only weakly stained. Grey matter (gm) was diffusely stained pink where AQP4 was normally expressed. (**B**) GFAP was diffusely stained at MS plaques and the normal appearing white matter. (**C**) These are typical MS lesions lacking MBP staining in the white matter (*). (**D**) With high magnification, the staining of GFAP was mesh-like, and many GFAP-stained hypertrophic astrocytes (arrows) and fibrous astrocytic foot processes were seen, and the staining was very strong at the pia mater and perivascular areas of the white matter lesions, where AQP4 was also stained (**E**) (mag $\times 200$). The loss of AQP4 and GFAP in NMO lesions with necrosis and cavities (**F** to **I**). (**F** to **H**) are serial sections of NMO3. This section includes heterogeneous stages of lesions, but were mainly of two types, 'actively demyelinating' (AD) and 'chronic active' (CA) lesions. AQP4 (**F**) and GFAP (**G**) were lost in disseminated lesions including these two types of lesions. MBP staining (**H**) was variably preserved. (**I**) and (**J**) are serial sections. (**I**) There are numerous GFAP-positive hypertrophic astrocytes (arrows) at the lesion edge and surrounding areas of the NMO lesions. In contrast, at the lesion centre, there were no morphologically typical fibrillary astrocytes positive for GFAP except for non-specific stainings like cell debris (arrowheads) in necrotic and cavitory lesions (cv), where AQP4 was completely lost (**J**) (mag $\times 200$).

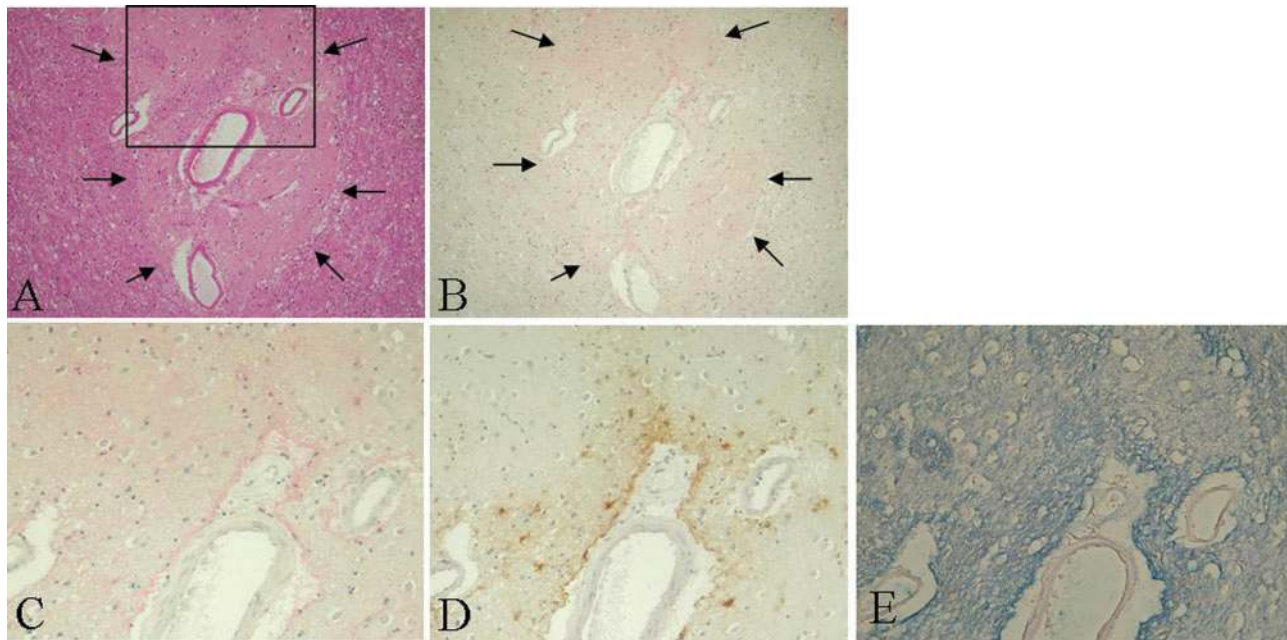


Fig. 5 The immunohistochemical features of acute infarction. **(A)** and **(B)** are serial sections of the acute phase of basal ganglia infarction. Around the blood vessel located in the centre, a necrotic lesion with eosinophilic appearance **(A)** in the area indicated with arrows is slightly positive for AQP4 **(B)** (mag $\times 100$). **(C to E)** are serial sections. At high magnification of the square shown in **(A)**, AQP4 was positive especially at the perivascular area **(C)**, and GFAP was similarly stained **(D)** (mag $\times 200$). **(E)** MBP was mostly preserved but there was pallor at the early necrotic areas (mag $\times 200$).

the NMO lesions lacking AQP4 and GFAP staining, it is suggested that complement-dependent cytotoxicity or antibody-dependent cell-mediated cytotoxicity, in which NMO-IgG, anti-AQP4 antibody, may be involved, might cause the degradation or downregulation of the water channel protein and eventually damage the astrocytes. It is unresolved what is the initial event or how serum anti-AQP4 antibody crosses the BBB and gains access to the antigen. However, our recent study on anti-AQP4 antibody in NMO showed that the patients' sera positively stained the cell surface of HEK 293 cells transfected with human AQP4 in a non-permeating condition (Takahashi *et al.*, 2006), indicating that serum anti-AQP4 antibody in NMO recognizes the extracellular domains of AQP4 protein. Thus, it is likely that anti-AQP4 antibody permeating through the BBB binds to AQP4 expressed on the surface of astrocytes to trigger the above-mentioned cytotoxic mechanisms in the perivascular regions of NMO. The primary breakdown of the BBB may allow the secondary influx of humoral or cellular immune components that attack the central nervous system, which could be the cause of the severe necrotic and cavitory lesions. In NMO lesions accompanied by necrotic and cavitory changes, loss of AQP4 and GFAP immunoreactivity was evident and reactive astrogliosis was poor. It is reported that a dysfunction of astroglial migration and delay of wound healing in astroglial monolayers *in vitro* occur in AQP4-deficient mice (Verkman *et al.*, 2006). Therefore, it is possible that the anti-AQP4 antibody may induce astroglial cell lysis, or

inhibit the migration and activation of astrocytes to repair the lesions.

Another important finding in the present study was the finding that MBP-stained myelinated fibres were relatively preserved in NMO lesions where AQP4 and GFAP immunoreactivities were widely lost. This is in contrast to the findings that immunoreactivity to myelin proteins such as MBP or myelin-associated glycoprotein was lost in plaques of MS (Itoyama *et al.*, 1980). A recent immunopathological study revealed that the perivascular deposition of activated complements and immunoglobulins is a feature of NMO that distinguishes it from MS (Lucchinetti *et al.*, 2002). Anti-AQP4 antibody might also be deposited in the perivascular region causing the loss of AQP4 immunoreactivity as well as the astrocytic impairment in NMO lesions. If anti-AQP4 antibody really plays a crucial role in the pathogenesis of NMO, it would be reasonable that myelins may be preserved or secondarily disturbed after astrocytes are widely destroyed in the process of tissue necrosis. At this point, it remains unknown how the loss of AQP4 might relate to tissue necrosis in NMO, but our data suggest that, unlike MS, inflammatory demyelination is not the primary pathological process in NMO.

Conclusions

In conclusion, the present study provides evidence of a unique pathogenesis in NMO, namely, astrocytic impairment associated with humoral immunity against AQP4 may

be primarily involved in NMO lesions. This pathomechanism is quite different from that of MS in which demyelination is the primary pathology. Further analyses using cell cultures and disease animal models are needed to clarify the basic mechanisms targeting AQP4 and astrocytes in NMO.

Acknowledgements

We wish to thank Dr Fusahiro Ikuta at Brain Research Center, Niigata Neurosurgical Hospital, who kindly gave us much advice, and Dr Kazuhiro Murakami at Tohoku Welfare Pension Hospital, who kindly provided materials for this study. We also wish to thank Mr Brent Bell for reading the manuscript. This work was supported by a grant-in-aid for young researcher (17790569) from the Ministry of Education, Culture, Sports, Science and Technology of Japan. Funding to pay the Open Access publication charges for this article was provided by Grant-in-aid of ministry of education, culture, sports, science and technology in Japan.

References

- Aoki-Yoshino K, Uchihara T, Duyckaerts C, Nakamura A, Hauw JJ, Wakayama Y. Enhanced expression of aquaporin 4 in human brain with inflammatory diseases. *Acta Neuropathol (Berl)* 2005; 110: 281–8.
- Ayers MM, Hazelwood LJ, Catmull DV, Wang D, McKormack Q, Bernard CC, et al. Early glial responses in murine models of multiple sclerosis. *Neurochem Int* 2004; 45: 409–19.
- Cloys DE, Netsky MG. Neuromyelitis optica. In: Viken PJ, Bruyn GW, editors. *Handbook of clinical neurology*. Vol. 9. Amsterdam: North-Holland; 1970. p. 426–36.
- Devic E. Myélite subaiguë compliquée de néurite optique. *Bull Med* 1894; 8: 1033–4.
- Gault F. De la neuromyérite optique aiguë [Thesis]. Lyon; 1894.
- Holley JE, Gveric D, Newcombe J, Cuzner ML, Gutowski NJ. Astrocyte characterization in the multiple sclerosis glial scar. *Neuropathol Appl Neurobiol* 2003; 29: 434–44.
- Itoyama Y, Sternberger NH, Webster HD, Quarles RH, Cohen SR, Richardson EP. Immunocytochemical observations on the distribution of myelin-associated glycoprotein and myelin basic protein in multiple sclerosis lesions. *Ann Neurol* 1980; 7: 167–77.
- Itoyama Y, Ohnishi A, Tateishi J, Kuroiwa Y, Webster HD. Spinal cord multiple sclerosis lesions in Japanese patients: Schwann cell remyelination occurs in areas that lack glial fibrillary acidic protein (GFAP). *Acta Neuropathol (Berl)* 1985; 65: 217–23.
- Jung J, Bhat R, Preston G, Guggino W, Baraban J, Agre P. Molecular characterization of an aquaporin cDNA from brain: candidate osmoreceptor and regulator of water balance. *Proc Natl Acad Sci USA* 1994; 91: 13052–6.
- Kira J. Multiple sclerosis in the Japanese population. *Lancet Neurol* 2003; 2: 117–27.
- Kuroiwa Y. Neuromyelitis optica (Devic's disease, Devic's syndrome). In: Koetsier JC, editor. *Handbook of clinical neurology*. Vol. 47. Demyelinating disease: Elsevier Science Publishers; 1985. p. 397–408.
- Lassmann H, Raine CS, Antel J, Prineas JW. Immunopathology of multiple sclerosis: report on an international meeting held at the institute of neurology of the university of Vienna. *J Neuroimmunol* 1998; 86: 213–17.
- Lennon VA, Kryzer TJ, Pittock SJ, Verkman AS, Hinson SR. IgG marker of optic-spinal multiple sclerosis binds to the aquaporin-4 water channel. *J Exp Med* 2005; 202: 473–7.
- Lennon VA, Wingerchuk DM, Kryzer TJ, Pittock SJ, Lucchinetti CF, Fujihara K, et al. A serum autoantibody marker of neuromyelitis optica: distinction from multiple sclerosis. *Lancet* 2004; 364: 2106–12.
- Lucchinetti CF, Mandler RN, McGavern D, Bruck W, Gleich G, Ransohoff RM, et al. A role for humoral mechanisms in the pathogenesis of Devic's neuromyelitis optica. *Brain* 2002; 125: 1450–61.
- Mandler RN, Davis LE, Jeffery DR, Kornfeld M. Devic's neuromyelitis optica: a clinicopathological study of 8 patients. *Ann Neurol* 1993; 34: 162–8.
- Misu T, Fujihara K, Nakamura M, Murakami K, Endo M, Konno H, et al. Loss of aquaporin-4 in active perivascular lesions in neuromyelitis optica: a case report. *Tohoku J Exp Med* 2006; 209: 269–75.
- Misu T, Fujihara K, Nakashima I, Miyazawa I, Okita N, Takase S, et al. Pure optic-spinal form of multiple sclerosis in Japan. *Brain* 2002; 125: 2460–8.
- Misu T, Fujihara K, Nakashima I, Sato S, Itoyama Y. Intractable hiccup and nausea with periaqueductal lesions in neuromyelitis optica. *Neurology* 2005; 65: 1479–82.
- Nakashima I, Fujihara K, Miyazawa I, Misu T, Narikawa K, Nakamura M, et al. Clinical and MRI features of Japanese patients with multiple sclerosis positive for NMO-IgG. *J Neurol Neurosurg Psychiatry* 2006; 77: 1073–5.
- Oshio K, Binder DK, Yang B, Schechter S, Verkman AS, Manley GT. Expression of aquaporin water channels in mouse spinal cord. *Neuroscience* 2004; 127: 685–93.
- Pittock SJ, Lennon VA, Krecke K, Wingerchuk DM, Lucchinetti CF, Weinschenker BG. Brain abnormalities in neuromyelitis optica. *Arch Neurol* 2006; 63: 390–6.
- Poser CM, Paty DW, Scheinberg L, McDonald WI, Davis FA, Ebers GF, et al. New diagnostic criteria for multiple sclerosis: guidelines for research protocols. *Ann Neurol* 1983; 13: 227–31.
- Takahashi T, Fujihara K, Nakashima I, Misu T, Miyazawa I, Nakamura M, et al. Establishment of a new sensitive assay for anti-human aquaporin-4 antibody in neuromyelitis optica. *Tohoku J Exp Med* 2006; 210: 307–13.
- Trapp BD, Peterson J, Ransohoff R, Rudick R, Mork S, Bo L. Axonal transection in the lesions of multiple sclerosis. *N Engl J Med* 1998; 338: 278–85.
- Verkman AS, Binder DK, Bloch O, Auguste K, Papadopoulos MC. Three distinct roles of aquaporin-4 in brain function revealed by knockout mice. *Biochim Biophys Acta* 2006; 1758: 1085–93.
- Vizuete ML, Venero JL, Vargas C, Ilundain AA, Echevarria M, Machado A, et al. Differential upregulation of aquaporin-4 mRNA expression in reactive astrocytes after brain injury: potential role in brain edema. *Neurobiol Dis* 1999; 6: 245–58.
- Wingerchuk DM, Hogancamp WF, O'Brien PC, Weinschenker BG. The clinical course of neuromyelitis optica (Devic's syndrome). *Neurology* 1999; 53: 1107–14.